revealed the remaining non-H atoms. Hydrogens of the phenyl and methylene groups were included at calculated positions with C temperature factors. The methyl H's were not found. Positional and anisotropic thermal parameters of non-H atoms were refined by full-matrix least squares. Programs used and other details have been listed previously.[8] Final agreement factors are $R_F = 0.040$ and $R_w = 0.038$ (0.067 and 0.039 including unobserved reflections). Positional parameters are listed in Table I.

Acknowledgment. We thank the National Science Foundation for an instrument grant (CHE-77893) toward the purchase of the FT-NMR spectrometer. We also thank Professor B. M. Foxman, Brandeis University, for help with Ortep.

Registry No. $Mo(CO)_5PPh_2P(O)(OEt)_2$, 102942-34-7; *cis*-$Mo(CO)_4[PPh_2P(O)(OEt)_2]_2$, 102942-35-8; $Mo(CO)_5PPh[P(O)(OEt)_2]_2$, 102942-36-9; $Mo(CO)_5P[P(O)(OEt)_2]_3$, 102942-37-0; *cis*-$Mo(CO)_4[P(OEt)_2OP(N\text{-}i\text{-}Pr_2)_2]$, 102942-38-1; $Fe(CO)_4P(N\text{-}i\text{-}Pr_2)_2P(O)(OEt)_2$, 102942-39-2; $Mo(CO)_5P(OEt)_2OP(N\text{-}i\text{-}Pr_2)_2$, 102942-40-5; $Mo(CO)_5P(NEt_2)_2P(O)(OEt)_2$, 102942-41-6; *cis*-$Mo(CO)_4[P(OEt)_2OP(NEt_2)_2]$, 102976-86-3; *cis*-$Mo(CO)_4(NHC_5H_{10})[PPh_2P(O)(OEt)_2]$, 102942-42-7; *cis*-$Mo(CO)_4(PPh_3)[PPh_2P(O)(OEt)_2]$, 102942-43-8; $NaMo(CO)_5P(OEt)_2O$, 90590-28-6; $Mo(CO)_6$, 13939-06-5; $Mo(CO)_4(NBD)$, 12146-37-1; diiron nonacarbonyl, 15321-51-4; (diethoxyphosphoryl)bis(diisopropylamino)phosphine, 102942-33-6; bis(diisopropylamino)chlorophosphine, 56183-63-2; diethyl phosphite, 762-04-9.

Supplementary Material Available: Tables of temperature factors, hydrogen atomic coordinates, and complete bond distances and angles (13 pages); a table of observed and calculated structure factors (39 pages). Ordering information is given on any current masthead page.

Contribution from the Department of Chemistry, University of Utah, Salt Lake City, Utah 84112,
and Department of Chemistry and Biochemistry, University of Guelph, Guelph, Ontario, Canada N1G 2W1

Magnetic Circular Dichroism of Cyclic π-Electron Systems. 28.[1] Sulfur-Nitrogen Heterocycles

Heinz-Peter Klein,[2a] Richard T. Oakley,[2b] and Josef Michl*[2a]

Received March 3, 1986

Electronic absorption and magnetic circular dichroism are reported for S_2N_2, S_4N_2, $S_3N_3O^-$, 1,5-*t*-$Bu_2C_2N_4S_2$, 1,5-$Ph_2C_2N_4S_2$, $S_4N_4O_2$, and two condensed-ring SN heterocycles, and linear dichroism is reported for S_4N_2 and one of the latter condensed-ring heterocycles. The results are analyzed in terms of the perimeter model and π-electron calculations.

Sulfur-nitrogen heterocycles have been an object of considerable interest in recent years.[3] In spite of their striking, vivid colors, attributed to $\pi^* \rightarrow \pi^*$ transitions,[4-15] relatively little is known about the assignment of their electronic excited states. Transition moment directions have been determined for only two of the molecules.[11] Magnetic circular dichroism was used to prove the degenerate nature of the lowest excited state of $S_3N_3^-$ [16] and to characterize the electronic transitions in two of its derivatives,[17] and its use in the case of the $S_4N_3^+$ cation doubled the number of assigned transitions.[18] It has been pointed out[5] that much more detailed information is needed for a reliable interpretation of the spectra in terms of quantum chemical calculations.

Chart I

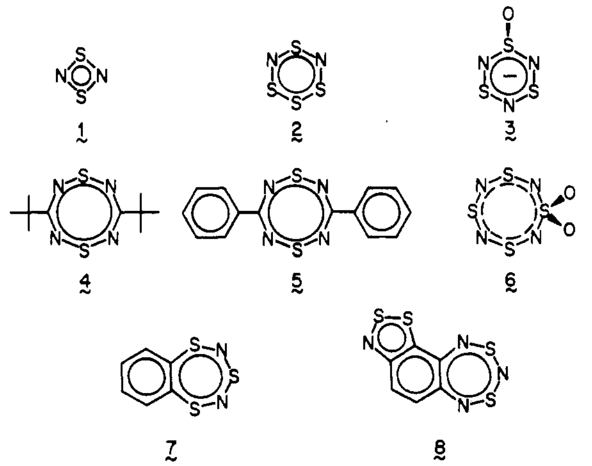

In the present paper we report the absorption and magnetic circular dichroism spectra of eight sulfur-nitrogen heterocycles **1-8** (Chart I) as well as the polarization directions of the electronic transitions in **2** and **7**. We find that the spectra can be interpreted remarkably well by means of the semiempirical π-electron PPP method,[19] which is generally recognized as successful for carbo-

---

(1) Part 27: Böttcher, A.; Raabe, G.; and Michl, J. *J. Org. Chem.* **1985**, *50*, 5050.

(2) (a) University of Utah. (b) University of Guelph.

(3) Chivers, T. *Chem. Rev.* **1985**, *85*, 341.

(4) Chivers, T.; Codding, P. W.; Laidlaw, W. G.; Liblong, S. W.; Oakley, R. T.; Trsic, M. *J. Am. Chem. Soc.* **1983**, *105*, 1186.

(5) Palmer, M. H. *Z. Naturforsch., A: Phys., Phys. Chem. Kosmophys.* **1983**, *38A*, 74.

(6) Bojes, J.; Chivers, T.; Laidlaw, W. G.; Trsic, M. *J. Am. Chem. Soc.* **1979**, *101*, 4517.

(7) Trsic, M.; Laidlaw, W. G. *Int. J. Quantum Chem., Quantum Chem. Symp.* **1983**, *17*, 367.

(8) Chivers, T.; Cordes, A. W.; Oakley, R. T.; Pennington, W. T. *Inorg. Chem.* **1983**, *22*, 2429.

(9) Trsic, M.; Laidlaw, W. G. *Inorg. Chem.* **1984**, *23*, 1981.

(10) Trsic, M.; Laidlaw, W. G.; Oakley, R. T. *Can. J. Chem.* **1982**, *60*, 2281.

(11) Gleiter, R.; Bartetzko, R.; Cremer, D. *J. Am. Chem. Soc.* **1984**, *106*, 3437.

(12) Cordes, A. W.; Marcellus, C. G.; Noble, M. C.; Oakley, R. T.; Pennington, W. T. *J. Am. Chem. Soc.* **1983**, *105*, 6008.

(13) Zahradník, R.; Banister, A. J.; Clarke, H. G. *Collect. Czech. Chem. Commun.* **1973**, *38*, 998.

(14) Bartetzko, R.; Gleiter, R. *Inorg. Chem.* **1978**, *17*, 995.

(15) (a) Burford, N.; Chivers, T.; Oakley, R. T.; Cordes, A. W.; Swepston, P. N. *J. Chem. Soc., Chem. Commun.* **1980**, 1204. (b) Burford, N.; Chivers, T.; Cordes, A. W.; Laidlaw, W. G.; Noble, M. C.; Oakley, R. T.; Swepston, P. N. *J. Am. Chem. Soc.* **1982**, *104*, 1282.

(16) Waluk, J. W.; Michl, J. *Inorg. Chem.* **1981**, *20*, 963.

(17) Waluk, J. W.; Chivers, T.; Oakley, R. T.; Michl, J. *Inorg. Chem.* **1982**, *21*, 832.

(18) Waluk, J. W.; Michl, J. *Inorg. Chem.* **1982**, *21*, 556.

cyclic π-electron systems. It was already noted previously that it performs well for the UV and MCD spectra of $S_3N_3^-$ [16] and $S_4N_3^+$.[18]

Since many of the sulfur–nitrogen heterocycles can be derived from a ($4N + 2$)-electron perimeter it is of interest to see whether their MCD spectra can be interpreted in terms of the perimeter model.[20] Previously[16–18] this was found to be the case for the four sulfur–nitrogen heterocycles whose MCD spectra were examined.

Experimental Section and Calculations

Materials. S_2N_2 (**1**) was prepared by passing S_4N_4 over silver wool.[21a] S_4N_4 was obtained by reduction of $S_4N_3^+Cl^-$ [21b] with iron turnings[21c] and was purified by sublimation. S_4N_2 (**2**),[4] $S_3N_3O^-$ (**3**),[8] *t*-$Bu_2C_2N_4S_2$ (**4**),[11] $Ph_2C_2N_4S_2$ (**5**),[22] $S_4N_4O_2$ (**6**),[23] $C_6H_4N_2S_3$ (**7**),[24] and $C_6H_2N_4S_4$ (**8**)[25] were prepared and purified according to the literature, except that **4** was purified by vacuum sublimation. The solvents used were of spectral grade.

Measurements. Absorption spectra were measured on a Cary 17 spectrophotometer, and magnetic circular dichroism spectra were measured on a Jasco 500C spectropolarimeter equipped with a 15 kG electromagnet. The Jasco 500C spectrophotometer was calibrated with the CD signal of *d*-camphorsulfonic acid[26a] and the MCD signal of naphthalene.[26b] The CD calibration was double-checked with the CD signals of D-pantolactone and Δ-(−)-$[Co(en)_3]I_3{\cdot}H_2O$.[26a] The spectra were digitized and plotted by using a PDP 11/23 microcomputer, which also calculated the oscillator strengths f and the B terms ($\beta_e D^2/cm^{-1}$) from $f = (4.319 \times 10^{-9})\int \epsilon \, d\tilde{\nu}$ and $B = -33.52^{-1}\int [\theta]_M/\tilde{\nu} \, d\tilde{\nu}$, where $\tilde{\nu}$ is the wavenumber, ϵ is the decadic molar extinction coefficient, and $[\theta]_M$ is molar ellipticity per unit magnetic field in deg L m^{-1} mol^{-1} G^{-1}.

The spectra of **2** and **4** were run in *n*-hexane, the spectra of **5** and **7** were run in acetonitrile, and the spectrum of **8** was run in methylene chloride. The solvents used for the measurements on **3** and **6** were methylene chloride (dried over P_2O_5) and acetonitrile (dried over P_2O_5 and distilled from CaH_2), respectively. Solutions of **3** and **6** were prepared by using standard vacuum line techniques (10^{-6} Torr).

The absorption and MCD spectra of **1** were run at 14 K on a thin layer of neat or argon-diluted material deposited on a CaF_2 window mounted on the cold end of an Air Products Displex CSA-202 closed-cycle cryostat. The matrix-isolation MCD apparatus was designed and constructed by Dr. K. A. Klingensmith and will be described elsewhere.[27]

The linear dichroic spectra of **2** and **7** were obtained in a stretched (~750%) polyethylene sheet by using the method of ref 28. The sheet was dipped in a chloroform solution of **7** for about 10 min, dried in air, and rinsed with methanol. Compound **2** was doped into the stretched polyethylene sheet from the gas phase at 18 °C over a period of 60 h. The linear dichroism of **7** was measured at room temperature and that of **2** at −196 °C on a sheet dipped into liquid nitrogen in a quartz Dewar vessel, in order to prevent evaporation losses. The spectra were recorded for two mutually perpendicular positions of a Glan polarizer located at 45° from the vertical, one with the electric vector of the light parallel and one with the electric vector perpendicular to the stretching direction of the sheet. A second polarizer was placed in the reference compartment. The absorption curves were digitized, the base lines obtained from the undoped polyethylene sheet were subtracted by computer, and the spectra were reduced to obtain the purely polarized components in the usual manner.[28]

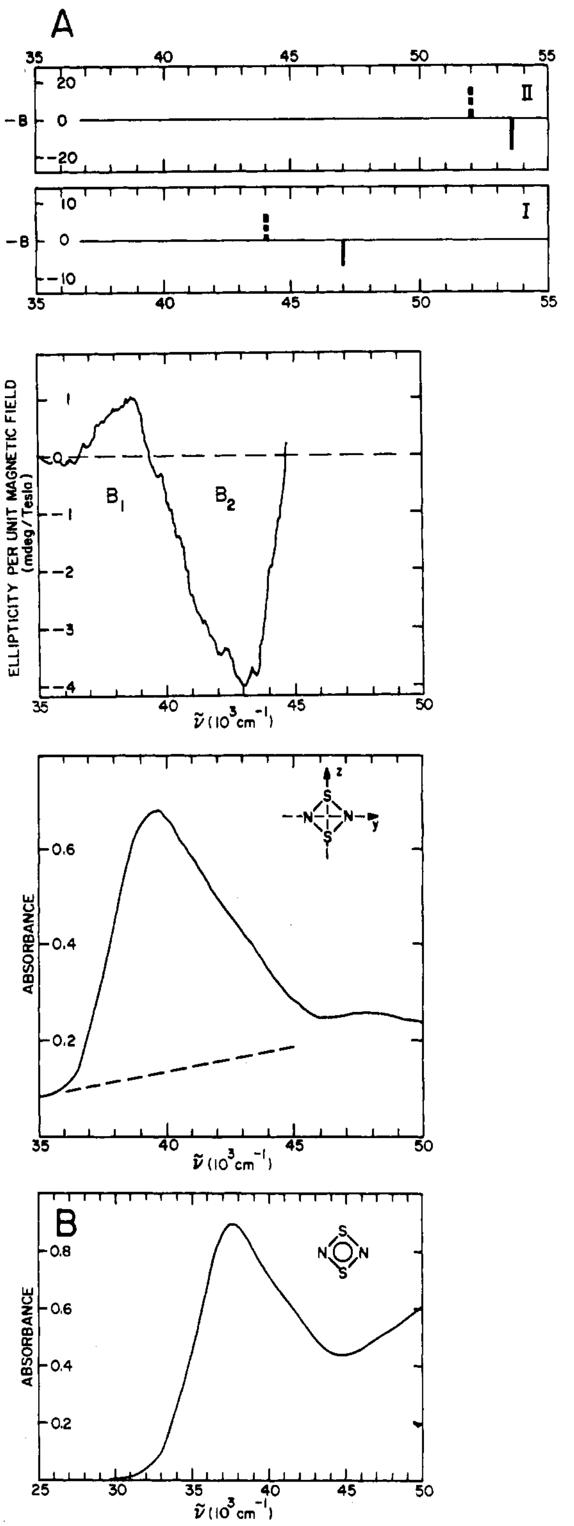

Figure 1. 1,3,2,4-Dithiadiazete. (A) From bottom to top: absorption in argon matrix; MCD in argon matrix at 14 K; calculation with parameter set I;[18,31] calculation with parameter set II.[11] Full bars indicate vertical polarization and broken bars indicate horizontal polarization with respect to the formula shown. The thickness of the bar is proportional to the calculated oscillator strength. (B) Absorption as neat film (14 K).

Calculations were performed by using the Pariser–Parr–Pople[19] (PPP) and INDO/S[29] methods, including all singly excited configurations. The INDO/S calculations gave very poor agreement with experiment, and the results have not been used further. The PPP calculations included next nearest neighbor interactions in the evaluation of the matrix ele-

---

(19) Pariser, R.; Parr, R. G. *J. Chem. Phys.* **1953**, *21*, 466, 767. Pople, J. A. *Trans. Faraday Soc.* **1953**, *49*, 1375.

(20) (a) Michl, J. *J. Am. Chem. Soc.* **1978**, *100*, 6801, 6812, 6819. (b) Michl, J. *Tetrahedron* **1984**, *40*, 3845.

(21) (a) Mikulski, C. M.; Russo, P. J.; Saran, M. S.; MacDiarmid, A. G.; Garito, A. F.; Heeger, A. J. *J. Am. Chem. Soc.* **1975**, *97*, 6358. (b) Jolly, W. L.; Maguire, K. D. *Inorg. Synth.* **1967**, *9*, 102. (c) Banister, A. J.; Fielder, A. J.; Hey, R. G.; Smith, N. R. M. *J. Chem. Soc., Dalton Trans.* **1980**, 1457.

(22) Ernest, I.; Holick, W.; Rihs, G.; Schomburg, D.; Shoham, G.; Wenkert, D.; Woodward, R. B. *J. Am. Chem. Soc.* **1981**, *103*, 1540.

(23) Roesky, H. W.; Schaper, W.; Petersen, O.; Müller, T. *Chem. Ber.* **1977**, *110*, 2695.

(24) (a) Morris, J. L.; Rees, C. W.; Rigg, D. J. *J. Chem. Soc., Chem. Commun.* **1985**, 396. (b) Cordes, A. W.; Hojo, M.; Koenig, H.; Noble, M. C.; Oakley, R. T.; Pennington, W. T. *Inorg. Chem.* **1986**, *25*, 1137.

(25) Codding, P. W.; Koenig, H.; Oakley, R. T. *Can. J. Chem.* **1983**, *61*, 1562.

(26) (a) Schippers, P. H.; Dekkers, H. P. J. M. *Anal. Chem.* **1981**, *53*, 778. (b) Vašák, M.; Whipple, M. R.; Michl, J. *J. Am. Chem. Soc.* **1978**, *100*, 6838.

(27) Klingensmith, K. A. Ph.D. Dissertation, University of Utah, 1985.

(28) Michl, J.; Thulstrup, E. W. *Spectroscopy with Polarized Light*; VCH: Deerfield Beach, FL, 1986. Thulstrup, E. W.; Michl, J.; Eggers, J. H. *J. Phys. Chem.* **1970**, *74*, 3868. Thulstrup, E. W.; Michl, J. *J. Am. Chem. Soc.* **1982**, *104*, 5594.

(29) Ridley, J.; Zerner, M. *Theor. Chim. Acta* **1974**, *32*, 111.

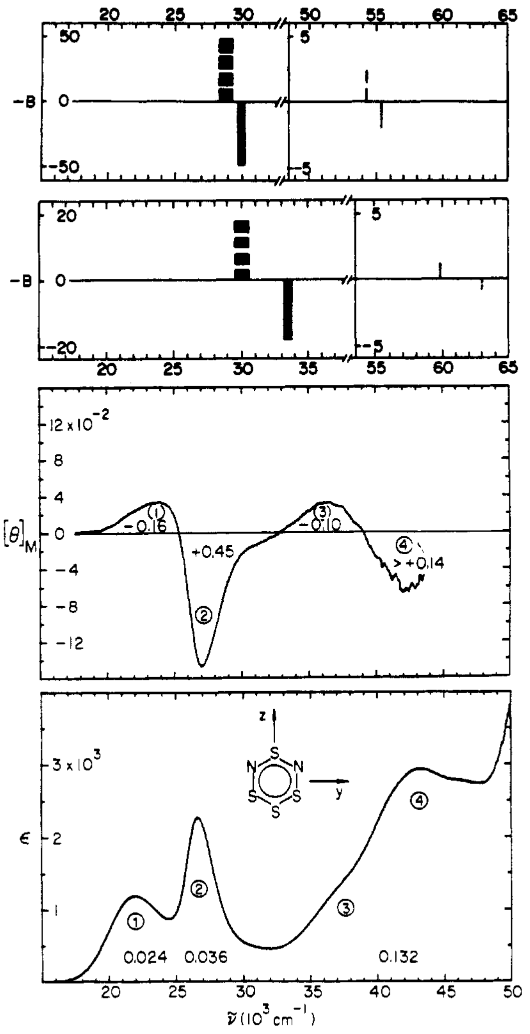

Figure 2. 1,2,3,5,4,6-Tetrathiadiazine. Solution absorption (oscillator strengths given) and MCD (B terms in units of $10^{-3}\beta_e D^2/\text{cm}^{-1}$).

ments of the magnetic moment operator[30] and were performed with two parameter sets. The first set (I) was I_C = 11.42 eV, A_C = 0.58 eV, I_N = 14.1 eV, A_N = 1.80 eV, I_{S+} = 20.27 eV A_{S+} = 10.47 eV, and β_{CC} = −2.318 eV, β_{CN} = −2.318 eV, β_{CS} = −1.62 eV, β_{SN} = −1.854 eV, and β_{SS} = −1.6 eV as used in our previous work.[18,31] The second set (II) was taken from ref 11 and differed in the values I_{S+} = 20.0 eV, A_{S+} = 9.16 eV, and β_{SN} = −2.31 eV. Two-center electron repulsion integrals were calculated according to the Mataga–Nishimoto formula.

In the following, we number the occupied MO's with positive integers starting with HOMO = 1 and the unoccupied MO's with negative integers starting with LUMO = −1.

Results and Discussion

The observed spectra are presented in Figures 1–8 and summarized in Table I.

1. π Systems Derived from 2π-Hole (4*N* + 2)-Electron Perimeters. The π-electron system of **1** contains six electrons in a [4]annulene perimeter and is isoelectronic with the $C_4H_4^{2-}$ dianion. The π systems of **2** and **3** contain 10 electrons in a [6]annulene perimeter and are isoelectronic with the $C_6H_6^{4-}$ tetraanion. Both $C_4H_4^{2-}$ and $C_6H_6^{4-}$ are representatives of the quite uncommon class of (4*N* + 2)-electron [2*N* + 2]annulenes, in which only two "holes" in the perimeter π orbitals remain unoccupied.[20]

The geometries of **2** and **3** are not fully planar; the sulfur atom in position 2 of **2**[4] is tilted by 54.9°, and the tricoordinate sulfur atom in **3**[8] is tilted by 43° above the S–N–S–N–S plane. Therefore, the cyclic conjugation in **2** and **3** will be diminished relative to an idealized planar system, but it will not vanish completely since there still is considerable overlap between the π-type AO's on the neighbors. Although the π and σ subsystems will now be coupled, we can still hope that a first-order description

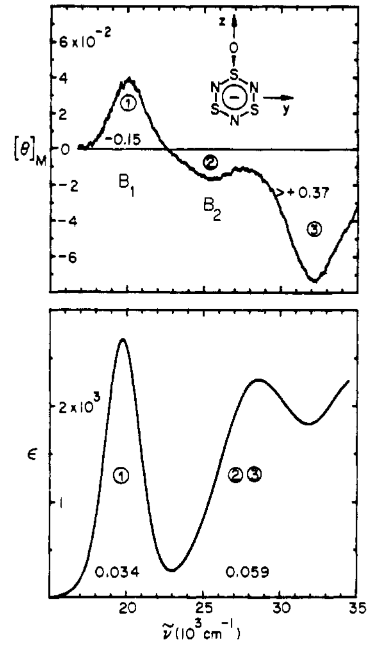

Figure 3. 1-Oxo-1,3,5,2,4,6-trithiatriazine anion (1−). See captions to Figures 1A and 2.

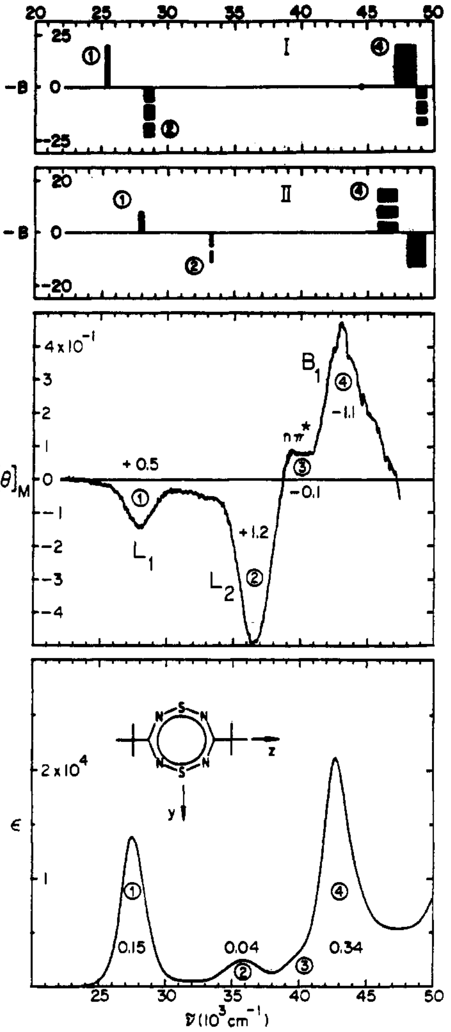

Figure 4. 3,7-Di-*tert*-butyl-1,5-dithia-2,4,6,8-tetrazocine. See captions to Figures 1A and 2.

---

(30) Jorgensen, N. H.; Pedersen, P. B.; Thulstrup, E. W.; Michl, J. *Int. J. Quant. Chem.* **1978**, *12*, 419.

(31) Castellan, A.; Michl, J. *J. Am. Chem. Soc.* **1978**, *100*, 6824.

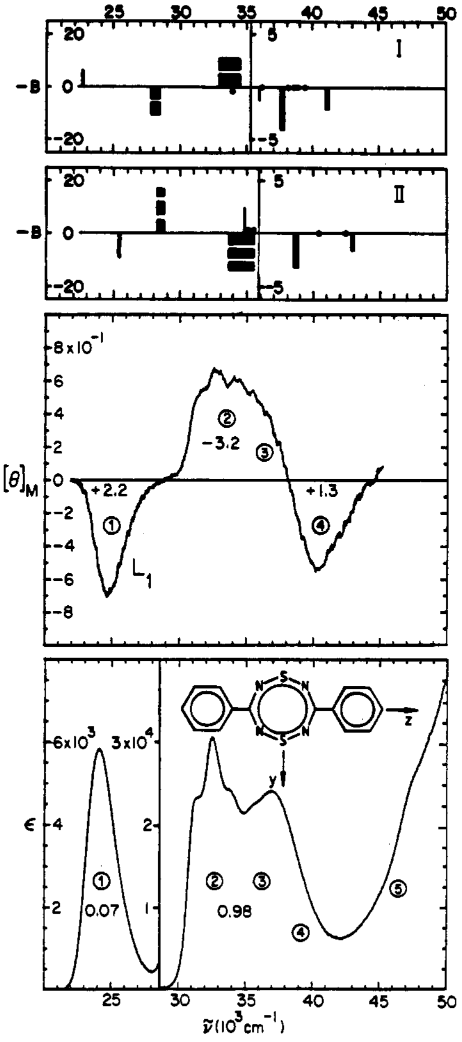

Figure 5. 3,7-Diphenyl-1,5-dithia-2,4,6,8-tetrazocine. See captions to Figures 1A and 2.

in terms of the perimeter model is possible. An encouragement can be derived from the fact that the MCD signs observed for two analogous compounds, S_3N_3–$NPPh_3$ and S_3N_3–$NAsPh_3$, agreed with expectations based on the perimeter model.[17]

In $(4N + 2)$-electron $[2N + 2]$annulenes HOMO is degenerate (orbitals 1 and 2) while LUMO is not (orbital −1). The low-energy $1,2 \rightarrow -1$ transition is doubly degenerate and is referred to as the B transition in the spirit of Platt's nomenclature. The LCAO version of the perimeter model predicts the A term of this transition to be negative and this agrees with the known spectra of species such as Se_4^{2+} (the free-electron version of the perimeter model fails in this case).[20]

In the case of the 2π-hole perimeters perturbed to a sufficiently low symmetry, the degeneracy of the B state is lifted. Two nondegenerate transitions, polarized in mutually perpendicular directions, are then expected. The lower one (B_1) corresponds to the $1 \rightarrow -1$ excitation, the upper one (B_2) to the $2 \rightarrow -1$ excitation. The perimeter model predicts a negative B term for B_1 and a positive one for B_2.[20]

S_2N_2 (1, Figure 1). The previously published absorption spectrum[32] contained a peak at 37 900 cm^{-1} (265 nm) and a shoulder at 32 300 cm^{-1} (310 nm). Our absorption spectra contain the peak but not the shoulder, which was therefore presumably due to a contaminant. The spectrum of the neat material is shown in Figure 1B. The argon-matrix spectrum shown in Figure 1A has a sloping base line due to scattering by the matrix. The absorption peak is shifted to 39 700 cm^{-1} (252 nm), a value similar to the ~250 nm value reported[33] in the gas phase.

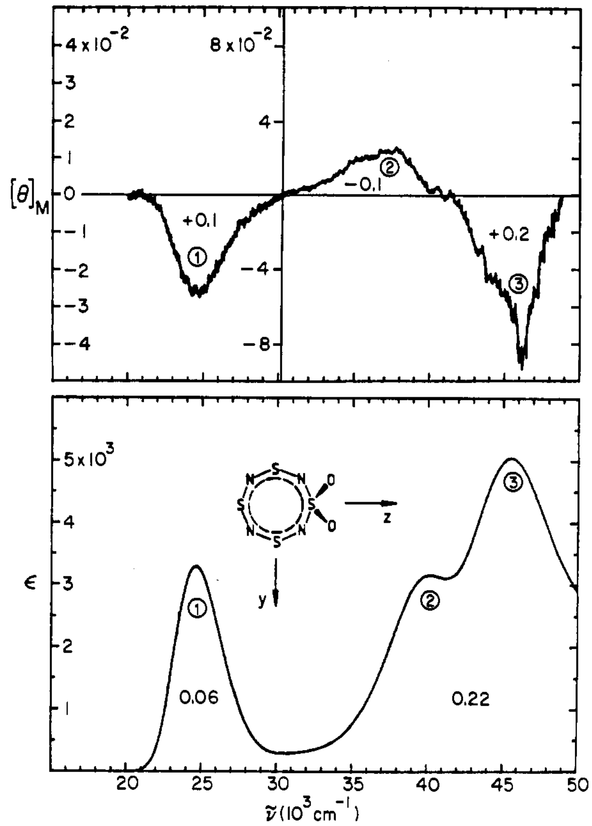

Figure 6. 1,1-Dioxo-1,3,5,7-tetrathia-2,4,6,8-tetrazocine. See captions to Figures 1A and 2.

In addition to the peak at 39 700 cm^{-1}, our argon-matrix spectrum shows an indication of a previously unreported shoulder near 43 000 cm^{-1}. A similar shoulder is present in the spectrum of the neat sample.

Two peaks are observed in the MCD spectrum. The first one corresponds to the peak in the absorption spectrum. It is centered near 39 000 cm^{-1} and has a negative B term. The strong second peak lies at 43 000 cm^{-1} and corresponds to the indistinct shoulder in the absorption curve. The B term is positive. Thus, the MCD spectrum leaves no doubt that the first absorption band of **1** consists of two electronic transitions.

Moreover, the results fit the anticipated behavior[20] exactly and represent reassuring verification of the MCD sign predictions obtained from the perimeter model.

The results obtained from the PPP model (Figure 1) reproduce the signs of the B terms of the observed two transitions as well. The calculated excitation energies are somewhat too high, though not as much as the previously published energies calculated for these transitions by an ab initio CI method.[34] We see no experimental evidence for the presence of an out-of-plane polarized transition at lower energies, predicted by these ab initio calculations. If it is present, it is very weak. In this regard, our results agree better with the prior INDO/S calculations,[35] which predict the first two transitions to be in-plane polarized ($\pi \rightarrow \pi^*$), albeit at much lower energies than observed experimentally.

S_4N_2 (2, Figure 2). The absorption spectrum shows the previously reported[4] bands at 22 000, 26 600, and 43 100 and a shoulder at 36 800 cm^{-1}. The first two low-energy transitions were assigned to the $1 \rightarrow -1$ and $2 \rightarrow -1$ $\pi^* \rightarrow \pi^*$ excitations on the basis of calculations by the transition-state method.[4] The MCD spectrum shows four B terms centered at the above energies with the signs −, +, −, and + in order of increasing energy. The observed linear dichroism shows that the band at 22 000 cm^{-1} is

---

[32] Iqbal, Z.; Downs, D. S. *Solid State Commun.* **1976**, *20*, 1147.

[33] Wiener, R. N.; Rubin, L. I.; Singh, S. N. *U.S. AEC* **1966**, *AFCRL-67-0512*, 491, 565; *Chem. Abstr.* **1969**, *71*, 96558.

[34] Jafri, J. A.; Newton, M. D.; Pakkanen, T. A.; Whitten, J. L. *J. Chem. Phys.* 1977, *66*, 5167.

[35] Millefiori, S.; Millefiori, A. *Inorg. Chim. Acta* **1980**, *45*, L19.

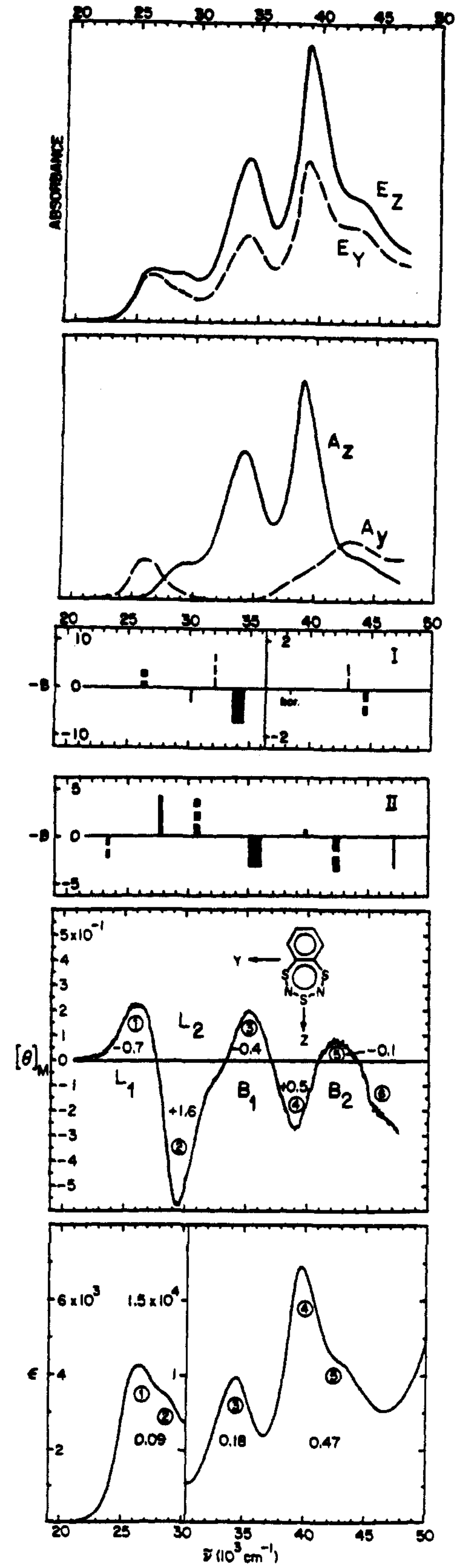

Figure 7. Benzo-1,3,5,2,4-trithiadiazepine. From bottom to top: absorption; MCD; calculations (see also captions to Figures 1A and 2); reduced absorption spectra with $A_z(\bar{\nu}) = E_Z(\bar{\nu}) - 1.08E_Y(\bar{\nu})$ (full line) and $A_Y(\bar{\nu}) = E_Y(\bar{\nu}) - 0.54E_Z(\bar{\nu})$ (dashed line); base line-corrected polarized absorption spectra for $E_Z(\bar{\nu})$ (full line) and $E_Y(\bar{\nu})$ (dashed line).

polarized perpendicular to and the band at 26 600 cm^{-1} parallel to the orientation axis of **2**. If the orientation is dictated by molecular shape in the usual way,[28] the absolute assignment of polarization directions is as shown in Table I. The degree of orientation is quite low, and we cannot confidently assign the polarizations in the region above 32 000 cm^{-1}.

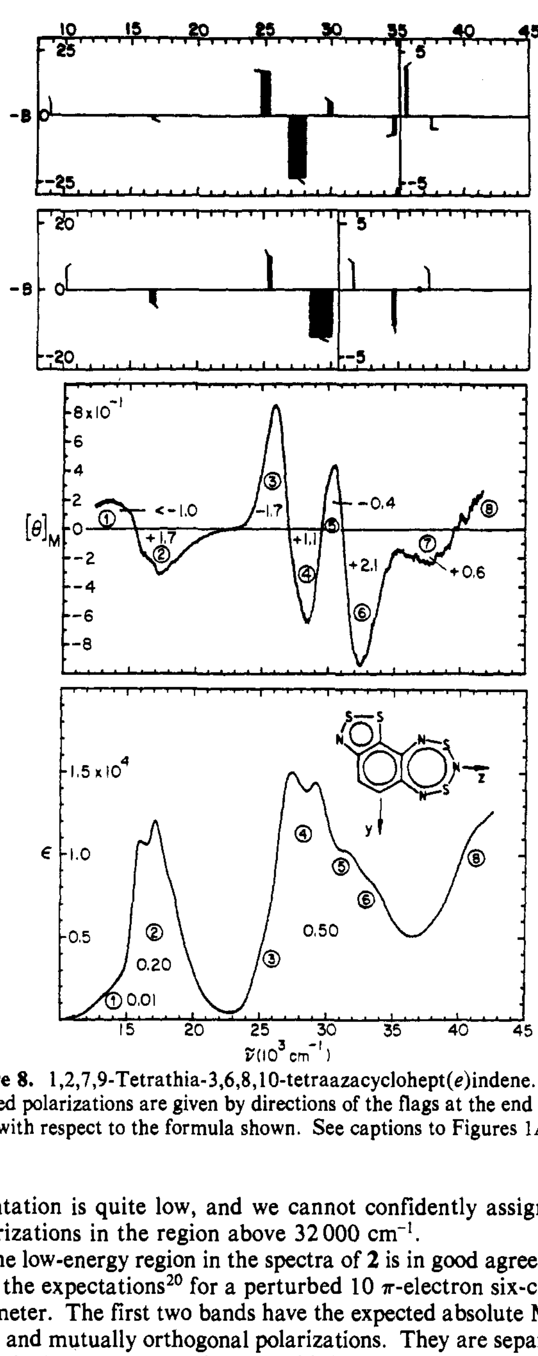

Figure 8. 1,2,7,9-Tetrathia-3,6,8,10-tetraazacyclohept(*e*)indene. Calculated polarizations are given by directions of the flags at the end of the bars with respect to the formula shown. See captions to Figures 1A and 2.

The low-energy region in the spectra of **2** is in good agreement with the expectations[20] for a perturbed 10 π-electron six-center perimeter. The first two bands have the expected absolute MCD signs and mutually orthogonal polarizations. They are separated by a sizable energy gap from the higher transitions, which are not described by the simple model. The results support the recently proposed[4] assignment of these low-energy transitions as π* → π*. A comparison with the extensive ab initio calculations of ref 5 is difficult since transition moments were not calculated, and it is hard to tell whether a calculated transition can be approximately described as π* → π* or n → π* or whether such an approximation is reasonable at all.

The results obtained by the PPP model in the π-electron approximation are shown on the top in Figure 2. They reproduce the polarization directions and the *B* terms of the first two transitions but produce excitation energies that are too high. The correct MCD signs are predicted also for the next two transitions, but the calculated energies are much too high. It is quite possible that weak transitions approximately described as due to *n*π* excitations also occur in this spectral region, but their presence is not obvious in our spectra.

$S_3N_3O^-$ (3, Figure 3). The absorption spectrum shows the recently reported[8] bands at 19 600 and 28 500 cm^{-1}. At energies above 35 000 cm^{-1} overlap with the absorption of the PPN$^+$ cation interferes and this region is therefore not shown. The *B* term of the first transition is negative. The MCD spectrum suggests

Table I
Electronic States of S-N Heterocycles[a]

Observed						Calculated (PPP)					
Compound	Transition	E(cm^{-1})	f	Pol.	B($10^{-3}\beta_e D^2$/cm^{-1})	E(cm^{-1})	f_p	f_r	Pol.	B($10^{-3}\beta_e D^2$/cm^{-1})	Dominant Configurations
1	1	38700			-7.5	50000	0.44	0.84	y	-12	1 → -1
	2	43000			+50	53500	0.50	0.72	z	+14	2 → -1
2	1	22000	0.024	y	-0.16	30100	0.43	0.95	y	-18.1	1 → -1
	2	26600	0.036	z	+0.45	33500	0.53	0.57	z	+18.4	2 → -1
	3	36800	0.13		-0.1	59900	0.04	0.04	z	-1.2	3 → -1
	4	43100			>+0.14	62900	0.01	0.08	y	+0.9	4 → -1
3	1	19600	0.034		-0.15						
	2	25500	0.059		+0.37						
	3	32200									
4	1	27600	0.15	y^b	+0.5	28100	0.10	0.34	y	-8.1	1 → -1
	2	35900	0.04	z^b	+1.2	33300	0.09	0.27	z	+11.3	2 → -1
	3	40000	0.34	x^b	-0.1						$n\pi^{*c}$
	4	42600		z^b	-1.1	46600	0.74	1.38	z	-16.5	1 → -2
						48800	0.56	1.36	y	+13.2	2 • -2
5	1	24100	0.07	y^b	+2.2	25500	0.04	0.19	y	+9.4	1 → -1
	2	32400	0.98	z^b	-3.2	28800	0.51	0.61	z	-17.2	1 → -2
	3	36900		z^b		34700	1.21	2.00	z	+13.8	2 → -1
						34900	0.001	0.002	y	-9.4	1 → -5, 1 • -4
						34900	0.00	0.00	y	-0.02	1 • -4, 1 • -5
						35500	0.00	0.00	z	0.0	1 • -3
	4	~40000		y^b	+1.3	38800	0.09	0.38	y	+3.2	2 → -2
						40500	0.00	0.00	y	0.0	2 → -3, 3 → -1
						42500	0.00	0.00	y	0.0	3 → -1, 2 • -3
	5	~47500		y^b	<0	43000	0.08	0.26	y	+1.6	1 → -5, 1 → -4
6	1	24600	0.06		+0.1						
	2	40000	0.22		-0.1						
	3	45500			+0.2						
7	1	26400	0.09	y	-0.7	23400	0.01	0.13	y	+2.3	1 → -1
	2	28800		z	+1.6	27700	0.13	0.15	z	-4.2	1 → -2
						30700	0.11	0.32	y	-3.9	1 → -3
	3	34400	0.18	z	-0.4	35600	0.67	0.91	z	+3.1	2 → -1, 2 → -3
	4	39700	0.47	z	+0.5	39800	0.25	0.32	z	-0.8	2 → -3, 2 • -1
	5	43000		y	-0.1	42400	0.21	0.50	y	+3.5	2 → -2
	6	~48000			>0	47300	0.08	0.11	z	+3.2	1 → -4, 3 → -2
8	1	14000	0.01		<-1.0	10200	0.002	0.03	40	-6.9	1 → -1
	2	17100	0.20		+1.7	16600	0.04	0.39	146	+3.9	2 → -1
	3	26000	0.50		-1.7	25400	0.05	0.29	118	-10.0	1 → -2, 2 → -2
	4	28400			+1.1	29300	0.60	1.73	157	+14.5	2 → -2, 1 • -2
	5	31400			-0.4	31600	0.01	0.04	141	-2.0	3 → -1
	6	33200			+2.1	34900	0.11	0.21	94	+2.7	1 → -3
	7	37800			+0.6	36700	0.002	0.001	148	+0.1	2 → -3, 4 → -1
	8	41400			<0	37400	0.03	0.04	146	-1.5	2 → -3, 1 → -4

[a] PPP calculations with parameter set II, f_p: oscillator length from dipole velocity, f_r: oscillator strength from dipole length; polarization angle (deg) counterclockwise from the z axis of formulas in Figures. [b] Experimental polarizations from ref. 11. [c] Assignment from Ref. 11.

strongly that the second band in the absorption spectrum is a superposition of at least two transitions, both of which have a positive *B* term.

The absorption and MCD spectra of **3** are very similar to those previously reported for the derivatives of the $S_3N_3^-$ anion,[17] $S_3N_3N{=}PPh_3$ and $S_3N_3N{=}AsPh_3$. The formal descriptions of the effects of the substitution on one of the sulfur atoms in $S_3N_3^-$ are similar in the three compounds[17]: (i) the tricoordinate sulfur will have a formal positive charge and increased effective electronegativity; (ii) the π system will be extended by interaction with the π orbitals of the ligand.

The LUMO and one of the HOMO's have an antinode at the position of substitution and therefore will be affected strongly by the substituent. Since monocoordinate oxygen is a good π donor, it will destabilize these two orbitals, particularly the HOMO, which is closer in energy. If the destabilizing effect of the oxygen does not exactly cancel the stabilizing effect of the increased electronegativity of the now tricoordinate sulfur, the degenerate HOMO–LUMO transition of $S_3N_3^-$ will be split into two transitions, one of which will be shifted to lower energies from the 28 000 cm^{-1} found in $S_3N_3^-$.[6]

The observed MCD signs of the B_1 and B_2 transitions are negative and positive, respectively,[17] and this agrees with the perimeter model. The transitions observed at higher energies cannot be interpreted readily within the framework of the qualitative model.

2. π Systems Derived from Other Charged [4*N* + 2]-Electron Perimeters. The heterocycles **4**–**6** are formally derived from a 10-π-electron 8-membered perimeter, while the ring systems of **7** and **8** originate in a 14-π-electron 11-membered and a 18-π-electron 14-membered perimeter, respectively. In a general charged $(4N + 2)$-electron [*n*]annulene perimeter $[N \neq 0, N \neq (n/2) - 1]$, both HOMO and LUMO are degenerate, and there are four possible single-electron excitations of the HOMO → LUMO type. They give rise to two doubly degenerate excited states, L at lower energies and B at higher energies. L transitions are forbidden by symmetry and appear in experimental spectra only due to vibronic mixing. B transitions are allowed and have a small *A* term.

If symmetry is lowered so that no threefold or higher axis of symmetry remains, the degeneracies of the L state and of the B state are removed. The intensities, polarizations, and MCD signs of the resulting four nondegenerate transitions, labeled L_1, L_2, B_1, and B_2 in order of increasing energy, are related to the nature of the perturbation in a relatively simple structure-sensitive way described in detail elsewhere.[20]

Each of the *B* terms of the four transitions of the perturbed annulene contains a contribution proportional to the out-of-plane component of the magnetic moment μ^- and a contribution proportional to the out-of-plane component of the magnetic moment μ^+, where μ^- and μ^+ are given by the difference and sum of the moments of an electron in the parent perimeter orbital of symmetry ϵ_{N+1} and an electron in the parent perimeter orbital of symmetry ϵ_N, respectively. For perimeters that contain about as many electrons as centers or fewer (positively charged perimeters), the μ^- moment is negative and small. In perimeters whose MO's are nearly all occupied in the ground state, the μ^- moment is positive and increases with the increasing negative charge on the perimeter. Theoretical estimates of μ^- are $+0.21\ \beta_e$ in $C_8H_8^{2-}$, $+0.27\ \beta_e$ in $C_{11}H_{11}^{3-}$, and $+0.30\ \beta_e$ in $C_{14}H_{14}^{4-}$. Roughly similar magnitudes can be expected for the S–N perimeters.[16] The values of μ^+ are all negative and more than an order of magnitude larger.

For a given perimeter, the contribution to a *B* term that is proportional to μ^- is insensitive to perturbations of molecular structure. Because of the smallness of μ^- relative to μ^+, it is important only if the μ^+ contribution vanishes or nearly vanishes (soft MCD chromophores). Otherwise, the μ^+ contribution is an order in magnitude larger than the μ^- contribution and alone determines the MCD signs. In contrast to the μ^- contribution, it is sensitive to the nature of the perturbation that produced the molecule of interest from the parent perimeter. This perturbation splits the originally degenerate HOMO and LUMO by amounts that are referred to as ΔHOMO and ΔLUMO, respectively. Their relative size can be frequently estimated by using first-order perturbation theory (PMO[36]), PPP, INDO/S, or ab initio calculations. The μ^+ contribution vanishes if ΔHOMO $\simeq$ ΔLUMO. Then, transition L_2 has a vanishing intensity in absorption and MCD. The μ^- contribution to the *B* term of L_1 is due to magnetic mixing of L_1 with B_1 states and its sign is opposed to that of μ^- and thus negative for our perimeters. This magnetic mixing makes a small positive μ^- contribution to the *B* term of the B_1 transition, while a B_1–B_2 magnetic mixing makes a larger negative one.

In only approximately soft chromophores, the L_2 transition will be weak but its intensity will no longer vanish. The sign of the μ^- contribution to its *B* term will then be given as a sum of a negative contribution from L_2–B_2 magnetic mixing and a positive one from L_2–L_1 magnetic mixing.

In MCD chromophores in which ΔHOMO $\neq$ ΔLUMO, the signs of *B* terms tend to be dictated solely by the μ^+ contributions. When ΔHOMO > ΔLUMO, these have the signs +, −, +, and − in order of increasing energy. Molecules that fulfill this condition are referred to as positive-hard chromophores. Molecules for which ΔHOMO < ΔLUMO holds are referred to as negative hard chromophores, and the signs of μ^+ contributions are −, +, −, and +. Each μ^+ contribution to a *B* term is again composed of two parts due to two pairwise magnetic field induced interactions between excited states. Their relative weight is affected by the energy separation between the two states. Magnetic mixing is particularly important for states of similar energy.

In the μ^+ contribution to the *B* term of the L_1 transition the effects of L_1–L_2 and L_1–B_1 kinds of mixing are opposed, the former normally dominating. In the case of the L_2 transition, the effects of L_2–L_1 and L_2–B_2 mixing reinforce each other. In the case of the B_1 transition the signs contributed by the B_1–L_1 and the B_1–B_2 magnetic mixing also agree.

***t*-Bu$_2$C$_2$N$_4$S$_2$ (4, Figure 4).** The absorption spectrum shows the recently reported[11] bands at 27 600, 35 900, and 42 600 cm^{-1} and a shoulder at 40 000 cm^{-1}. The MCD spectrum shows four *B* terms, centered at these energies, with the signs +, +, −, and −. The strong absorption band has been previously assigned to $\pi \rightarrow \pi^*$ transitions and the shoulder at 40 000 cm^{-1} to a $n \rightarrow \pi^*$ transition based on polarization measurements and on ab initio calculations on the parent 1,5-dithia-2,4,6,8-tetrazocine.[11]

The assignment of the three observed π-π^* transitions as L_1, L_2, and B_1 in order of increasing energy is straightforward when one considers the known polarization directions (Table I).[11] The parallel polarization of the second (L_2) and fourth (B_1) bands makes it clear that their *B* terms do not originate from their mutual magnetic mixing although this would be suspected upon a superficial inspection of Figure 4.

The weakness of the L_2 absorption suggests that ΔHOMO and ΔLUMO are not very different. However, the observed *B* terms cannot be assigned as due to μ^- contributions alone. Although that of the B_1 transition is strongly negative as expected for a perimeter whose μ^- moment is positive, the signs of the *B* terms of L_1 and L_2 are not negative.

The signs of all three *B* terms can be understood if ΔHOMO − ΔLUMO is hypothesized to be weakly negative, so that μ^+ contributions from the magnetic mixing are present. For the L_2 transition, the L_2–L_1 and L_2–B_2 types of mixing make a positive contribution, resulting in the observed positive *B* term. For the B_1 transition, both B_1–L_1 and B_1–B_2 make a negative μ^+ contribution, reinforcing that from the μ^- contribution and resulting in the observed negative *B* term. In the case of the L_1 transition, the μ^+ contribution due to L_1–L_2 mixing is negative and that due to L_1–B_1 mixing is positive. In the simple model, the former always prevails since the L_1–L_2 energy separation is maller than that for L_1–B_1. However, in **4** the L_1–L_2 separation is unusually large and almost equal to the L_1–B_1 separation. Although in the simple model the relative weights of these two contributions are determined strictly by the energy denominators, this is apparently not always true in reality and in the case of **4** the L_1–B_1 magnetic mixing just barely dominates over the L_1–L_2 mixing to produce a net weakly positive *B* term for the L_1 transition.

The use of the PMO theory[36] on the symmetry-determined perimeter MO's as well as the use of PPP and INDO/S calculations all yield a negative ΔHOMO − ΔLUMO value and thus support the above proposal. Note that the opposite assumption, ΔHOMO > ΔLUMO, would account for the weakly positive *B* term of the L_1 band but cannot account for the much stronger positive *B* term of the L_2 band (the experimental polarizations guarantee that the latter is not due to a mixing with the fourth observed transition, either.)

However, the numerical PPP computations of the *B* terms do not yield the correct positive sign for the L_1 transition. We suspect that this is caused by the exaggerated separation of the L and B bands and the vastly underestimated separation of the L_1 and L_2 bands in the computed spectrum (Figure 4). This favors the L_1–L_2 mixing and disfavors the L_1–B_1 mixing in the computed MCD spectrum, leading to the wrong sign for L_1 but still the correct signs for L_2 and B_1. The parameter set II is somewhat better than set I in that it produces more realistic energy gaps, orders the B_1 and B_2 states correctly, and yields comparable

---

(36) Dewar, M. J. S.; Dougherty, R. C. *The PMO Theory of Organic Chemistry*; Plenum: New York, 1975.

intensities for the L_1 and L_2 absorptions. Indeed, it also produces a less negative B term for the L_1 transition. We suspect that a parameter choice that would reproduce the energy gaps and ΔHOMO–ΔLUMO value correctly would yield correct MCD signs and absorption intensities, but have not engaged in such a parameter search. In this regard, it is quite discouraging to note that for **7** the parameter choice II is inferior to choice I (see below).

$Ph_2C_2N_4S_2$ (5, Figure 5). In view of the complications in the interpretation of the MCD spectrum of **4**, it appeared worthwhile to examine an additional derivative of the $C_2N_4S_2$ ring system. The absorption spectrum of **5** shows the recently reported[22] bands at 24 100, 32 400, and 36 900 cm^{-1} and a shoulder at 47 500 cm^{-1}. Linear dichroism revealed that a further transition is present near 40 000 cm^{-1} and overlaps considerably with the transition at 36 900 cm^{-1}. The MCD spectrum shows three strong bands in the region up to 45 000 cm^{-1}, with the signs +, –, and +. The broad band near 34 000 cm^{-1} is a superposition of contributions from the two transitions at 32 400 and 36 900 cm^{-1}. Both transitions have a negative B term. The proposed assignments of the three bands labeled 1, 2, and 3 in Figure 5 are L_1, L_2, and B_1, respectively. A comparison of the spectra of **4** and **5** shows that the extension of conjugation due to the presence of two phenyl rings can hardly be viewed as a minor perturbation. Insofar as the perimeter model still can be applied, it suggests that in **5** the ΔHOMO – ΔLUMO difference is positive.

The results of PPP calculations for **5** depend on the choice of parameters. With set II we obtain ΔHOMO > ΔLUMO and the expected B term signs for the first two transitions (+, –). With set I we obtain ΔHOMO < ΔLUMO and a corresponding reversal of B term signs (–, +). The former agree with the observed signs.

$S_4N_4O_2$ (6, Figure 6). The absorption spectrum has apparently not been published before. It shows three transitions at 24 600, 40 000, and 45 500 cm^{-1}. The MCD spectrum shows three B terms centered at these energies. The signs of the B terms are +, –, and + in order of increasing energy.

Assuming hyperconjugation through a low-lying π-symmetry orbital of the SO_2 group, **6** can be treated in terms of the perimeter model. The spectrum is then readily analyzed in terms of the L_1, L_2, and B_1 transitions, with a small positive value of ΔHOMO – ΔLUMO. This will produce relatively weak μ^+ contributions with signs +, –, and + for the B terms in order of increasing energy and μ^- contributions with –, –, and + signs, accounting for the observed MCD signs and intensities (note that the μ^- moment is positive for this perimeter and compare the similar analysis for t-$Bu_2C_2N_4S_2$ given above). The PPP method is not readily applicable to **6**, and no INDO/S parameters for an S–O combination are available at present. However, we have checked that a small positive value of ΔHOMO – ΔLUMO is compatible with the simple PMO theory.[36]

$C_6H_4N_2S_3$ (7, Figure 7). The absorption spectrum shows the recently reported[24] bands at 26 400, 34 400, and 39 700 cm^{-1} and two shoulders at 28 800 and 43 000 cm^{-1}. The MCD spectrum shows five bands located at these energies and reveals a sixth band at about 48 000 cm^{-1}. The MCD signs of the six B terms are –, +, –, +, –, and + in order of increasing energy. The linear dichroism of **7** shows that the transitions at 26 400 and 43 000 cm^{-1} are polarized perpendicular and the transitions at 28 800, 34 400 and 39 700 cm^{-1} parallel to the orientation axis. From previous experience[28] with the relation between molecular shape and orientation, it is safe to assume that the long axis is the z axis shown in Figure 7.

Interpretation of the spectra was based on PPP calculations, with parameter sets I and II used again. The calculations with parameter set I suggest that the four perimeter orbitals relevant to the problem do not represent the four frontier MO's of **7** because an "intruder" orbital is interleaved with them under the effect of the perturbation. According to these PPP calculations, orbitals 2 and 1 originate in the HOMO orbital pair of the $C_{11}H_{11}^{3-}$ perimeter (ϵ_3, ϵ_{-3}), orbitals –1 and –3 in the LUMO orbital pair of $C_{11}H_{11}^{3-}$ (ϵ_4, ϵ_{-4}), while the orbital –2 originates in the next higher pair of perimeter orbitals (ϵ_5, ϵ_{-5}). The usual ΔLUMO quantity must therefore be obtained as the difference of the energies of MO's –1 and –3, and this type of situation demonstrates the inherent limitations of the perimeter model.

The two sets of calculations both provide a fairly decent fit of the observed transition energies and polarizations if it is assumed that the third transition, polarized along the y axis, is too weak to be observed. It is indeed calculated to be very weak with parameter set I, but not with set II. Both calculations badly underestimate the intensity of the z-polarized transition 4. The wave functions have the proper form for the identification of the first, second, third, and fifth observed transitions as L_1, L_2, B_1, and B_2, respectively. The unobserved third calculated transition involves an excitation into the "intruder" orbital, as does the observed fourth transition (actually, B_1 character is shared with "intruder-state" character in both the third and fourth observed transitions).

The two sets of calculations differ considerably in the computed MCD properties, with parameter set II distinctly inferior to set I. The former yield ΔHOMO > ΔLUMO and incorrect MCD signs for almost all transitions. The latter yield ΔHOMO slightly smaller than ΔLUMO and all correct MCD signs except for that of the third transition. This great sensitivity of the MCD results to minor details of the parameterization choice illustrates both its value in the testing of computed wavefunctions and the difficulties encountered in the computation MCD spectra of complicated molecular systems.

Note that the L_1 and L_2 signs are in agreement with ΔHOMO < ΔLUMO in terms of the perimeter model; the magnitude of this difference is probably somewhat underestimated even by the better of the two calculations. The positive sign of the third observed transition may be due to a μ^- contribution, notoriously difficult to handle properly in a PPP calculation.

$C_6H_2N_4S_4$ (8, Figure 8). The absorption spectrum shows the recently reported[25] bands at 17 100 and 28 400 cm^{-1} and shoulders at 14 000, 26 000, 31 400 and 33 200 cm^{-1}. The MCD spectrum clearly reveals the presence of eight bands. The first six bands are centered at the above energies, and the last two bands are located near 37 800 and 41 400 cm^{-1}, respectively. The MCD signs of the B terms, in order of increasing energy, are –, +, –, +, –, +, +, and –. The relative splitting of the originally degenerate pairs of the parent perimeter HOMO's and LUMO's was calculated by the PPP method. The result is a small splitting of the HOMO's and a large splitting of the LUMO's, and **8** should be a negative hard chromophore. The MCD signs of the four low-energy transitions, labeled L_1, L_2, B_1, and B_2, are then expected to be –, +, –, and +, in perfect agreement with experiment. With either parameter choice, I or II, the PPP model reproduces the observed energies, relative oscillator strengths, and MCD signs of the first six bands very well.

Conclusions

The electronic states and magnetic circular dichroism of eight S–N heterocycles have been characterized and analyzed in terms of the perimeter model and π-electron calculations. The energies, absorption intensities, and polarizations of the first few electronic transitions can be accounted for nicely in terms of $\pi^* \rightarrow \pi^*$ excitations. The MCD spectra are of considerable help in uncovering otherwise partially or completely hidden transitions. The MCD signs of the simpler systems are readily related to the structural formula by using simple concepts of the perimeter model. For the more complex ones, they can be calculated fairly successfully by the PPP method, but some difficulties and ambiguities have been encountered with parameter choice. Their resolution continues to pose a theoretical challenge. However, it is noteworthy that the simple perimeter model and the PPP method perform as well as they do for these complex inorganic ring systems.

Acknowledgment. This work was supported by U.S. Public Health Service Grant IR01-GM 32773. We are indebted to Dr. K. A. Klingensmith for assistance. H.-P.K. is grateful for a NATO scholarship granted through the DAAD.

Registry No. **1**, 25474-92-4; **2**, 57970-08-8; **3**, 81260-53-9; **4**, 89909-08-0; **5**, 76843-75-9; **6**, 57932-64-6; **7**, 97484-08-7; **8**, 87605-08-1.